



UNIVERSITY OF LEEDS

This is a repository copy of *Improved Understanding of Cefixime Trihydrate Reactive Crystallization and Process Scale-up with the Aid of PAT*.

White Rose Research Online URL for this paper:  
<http://eprints.whiterose.ac.uk/149568/>

Version: Accepted Version

---

**Article:**

Yu, S, Zhang, Y and Wang, XZ (2019) Improved Understanding of Cefixime Trihydrate Reactive Crystallization and Process Scale-up with the Aid of PAT. *Organic Process Research and Development*, 23 (2). pp. 177-188. ISSN 1083-6160

<https://doi.org/10.1021/acs.oprd.8b00190>

---

© 2019, American Chemical Society. This document is the Accepted Manuscript version of a Published Work that appeared in final form in *Organic Process Research and Development* © American Chemical Society after peer review and technical editing by the publisher. To access the final edited and published work see <https://doi.org/10.1021/acs.oprd.8b00190>.

**Reuse**

Items deposited in White Rose Research Online are protected by copyright, with all rights reserved unless indicated otherwise. They may be downloaded and/or printed for private study, or other acts as permitted by national copyright laws. The publisher or other rights holders may allow further reproduction and re-use of the full text version. This is indicated by the licence information on the White Rose Research Online record for the item.

**Takedown**

If you consider content in White Rose Research Online to be in breach of UK law, please notify us by emailing [eprints@whiterose.ac.uk](mailto:eprints@whiterose.ac.uk) including the URL of the record and the reason for the withdrawal request.



[eprints@whiterose.ac.uk](mailto:eprints@whiterose.ac.uk)  
<https://eprints.whiterose.ac.uk/>

1 PAT Aided Identification of Operational Spaces Leading to  
2 Tailored Crystal Size Distributions in Azithromycin  
3 Crystallization via Coordinated Cooling and Solution Mediated  
4 Phase Transition

5

6 Xi H. Tang<sup>a</sup>, Yang Li<sup>a</sup>, Jing J. Liu<sup>a</sup>, Yang Zhang<sup>a\*</sup> and Xue Z. Wang<sup>a,b\*</sup>

7

8

9

10 <sup>a</sup> Engineering Center for Pharmaceutical Process Innovation and Advanced Process  
11 Control of Guangdong Province, School of Chemistry and Chemical Engineering,  
12 South China University of Technology, Guangzhou, Guangdong, PR China, 510640

13

14 <sup>b</sup> School of Chemical and Process Engineering, University of Leeds, Leeds LS2 9JT,  
15 UK.

16

17

18

19

20

21 \* Correspondence authors, Professor Xue Z. Wang and Dr Yang Zhang:

22 E-mails: xuezhongwang@scut.edu.cn, or [x.z.wang@leeds.ac.uk](mailto:x.z.wang@leeds.ac.uk);

23 ceyzhang@scut.edu.cn

24 Tel.: +86 (20) 87114000, or +44 (0) 113 3432427; +86(20)87114050

25

26

27

28

1 **Abstract**

2

3 On-line imaging and ATR-FTIR were applied to azithromycin crystallization in a  
4 mixture of acetone and water to identify the operational spaces that consistently led to  
5 tailored crystal size distribution (CSD) in the size ranges of  $< 180 \mu\text{m}$  ( $D_{50} = 78.3 \mu\text{m}$ ),  
6  $180 - 425 \mu\text{m}$  ( $D_{50} = 155 \mu\text{m}$ ) and  $425 - 850 \mu\text{m}$  ( $D_{50} = 433 \mu\text{m}$ ), under the  
7 constraints of no change of solvent or addition of crystal growth modifiers, in the  
8 meantime satisfying all other specifications including drug stability, purity, impurity  
9 content, and avoidance of monohydrates in the dihydrate crystals. Azithromycin  
10 crystallization in acetone and water mixture is both interesting and challenging as it  
11 achieves crystallization via coordinated manipulation of two variables: introduction of  
12 water as an anti-solvent and temperature reduction via cooling. While the target  
13 product crystals are azithromycin dihydrates, it can only firstly produce monohydrates  
14 which are then transformed to dihydrates through solution mediated phase transition  
15 (SMPT). The phenomenon of SMPT from monohydrates to dihydrates was visually  
16 observed in real-time using an online imaging probe and the factors affecting the  
17 transition were identified and quantified using the ATR-FTIR. Furthermore, it was  
18 found that the way water was introduced could affect the hydrate transition and the  
19 crystal size distribution of the product. Based on the understanding of the causal  
20 relationships between the multiple variables and crystal growth behavior, the  
21 operational spaces leading to the three desired CSDs were defined. The results were  
22 firstly obtained in a 1 L crystallizer, and then validated in a 25 L crystallizer.

23

24 **Keywords:** azithromycin crystallization; process analytical technology; tailored  
25 crystal size distributions; solvent mediated phase transition; polymorphism; scale-up

## 1 **1. Introduction**

2 Azithromycin (CAS No. 83905-01-5), also known as Zithromax, is the first  
3 semi-synthetic 15-membered ring aza-macrolide antibiotic, obtained by structural  
4 modification of erythromycin.<sup>1</sup> Compared with erythromycin, azithromycin is more  
5 stable under acidic condition with an extended spectrum of antibacterial activity and  
6 more desirable pharmacokinetic properties.<sup>2</sup> It is mainly used for the treatment of  
7 respiratory tract and urinary tract infections, skin and soft tissue infections and simple  
8 genital infections. Due to its long half-life, reduced dosing frequency, shorter course  
9 of treatment and low incidence of adverse reactions, it is still recommended as the  
10 first-line treatment for the above infections by a number of national and regional  
11 medical guidelines.<sup>3,4</sup>

12 Azithromycin has a variety of solvates, among which hydrates have been studied  
13 and used most widely. According to the difference in water content, azithromycin has  
14 four major crystal forms: dehydrates, monohydrates, dihydrates<sup>5-7</sup> and sesquihydrates  
15 existing under certain conditions.<sup>8</sup> In commercially available solid formulations,  
16 azithromycin mainly exists in the form of dihydrate crystals produced in a mixture of  
17 acetone and water.<sup>9</sup>

18 The dilution crystallization of azithromycin is a very interesting but challenging  
19 industrial process. Customers demand three crystal size ranges, < 180  $\mu\text{m}$ , 180 – 425  
20  $\mu\text{m}$  and 425 – 850  $\mu\text{m}$ . Efforts were made to develop the crystallization process for  
21 manufacturing azithromycin crystals with desired crystal size distributions (CSDs).<sup>10</sup>  
22 However, previous efforts failed in producing crystals of the size range 425 – 850  $\mu\text{m}$   
23 directly through crystallization using the mixture of acetone and water as the solvent,  
24 unless the solvent was changed. Solvent change was constrained by administrative  
25 and environmental considerations as well as cost. Azithromycin dilution  
26 crystallization has two manipulated variables, water addition as an anti-solvent and  
27 temperature reduction via cooling. It was reported that although dihydrate crystals are  
28 the desired product, monohydrates are always firstly formed and then converted to  
29 dihydrates through polymorph transition in the mixture of acetone and water.<sup>11</sup> The

1 transition process is hard to control and the desired CSD of the final product is not  
2 guaranteed. Some previous publications and patents reported methods to make  
3 smaller-sized azithromycin dihydrates with a certain degree of agglomeration,<sup>11-15</sup> but  
4 obtaining larger-sized particles via direct crystallization in a mixture of acetone and  
5 water remains an unresolved challenge.

6 Optimization of crystallization conditions can be achieved via simulation if  
7 reliable models are available. Otherwise, it has to rely on experiments. To speed up  
8 the process of experiment based approach to optimization of crystallization conditions,  
9 PAT (Process Analytical Technology) instrument should be used. PAT instrument  
10 studied for crystallization includes ATR-FTIR, online imaging, ultrasound, and  
11 Raman; and the work has been reviewed in some review and research articles.<sup>16-23</sup> In  
12 this work, on-line imaging and ATR-FTIR were used to find and define the  
13 operational envelopes leading to desired CSDs. The PAT instrument was applied  
14 during experiments to qualitatively and quantitatively characterize the crystal growth  
15 of azithromycin and polymorph transition and study the effects of several variables  
16 including the addition of water as an anti-solvent, temperature, and stirrer speed.  
17 Consequently, the operational spaces leading to desired product CSDs were defined.  
18 The operational spaces were firstly derived from a 1 L crystallizer, and then validated  
19 in a 25 L crystallizer.

20

## 21 **2. Materials and Methods**

### 22 **2.1. Materials**

23 Azithromycin dihydrate was provided by a pharmaceutical company that  
24 sponsored the work (name not disclosed in this paper due to nondisclosure agreement  
25 signed with the company). Acetone (AR) was purchased from Guangzhou Chemical  
26 Reagent Factory, China. The solvent was used without further purification. Deionized  
27 water was produced by an ultrapure water system.

28

29

1

## 2 **2.2. Processes, Optimization Objectives and PAT instrument**

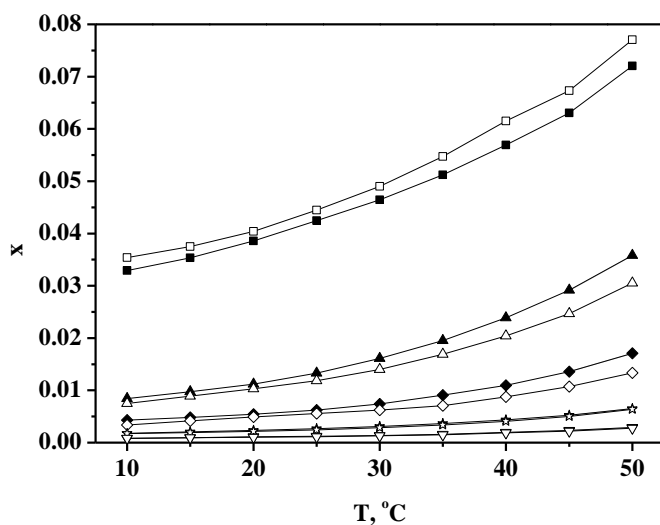
### 3 2.2.1 Azithromycin Crystallization in Acetone/water Mixture

4 At present, the commercially valuable azithromycin product is mainly in the  
5 form of dihydrate crystals manufactured mainly via cooling and dilution  
6 crystallization in the mixture of acetone and water. Firstly, crude azithromycin  
7 product is dissolved in pure acetone at a certain temperature. Then, the first portion of  
8 water as an anti-solvent is introduced to the solution until crystals are observed.  
9 Monohydrate crystals are formed first and the temperature is kept constant for several  
10 hours until the crystals are transformed to dihydrates. After that, the temperature is  
11 reduced to a certain value and the second portion of water is added at a slow rate in  
12 order to increase the final yield. The complexity of the process is mainly due to the  
13 need for coordinated optimization of multiple parameters: cooling rate, the amount of  
14 water and the water addition rate. Moreover, it is necessary to avoid incomplete  
15 hydrate transition or no hydrate transition. The products of the processes need to meet  
16 the three CSD requirements of customers:  $< 180 \mu\text{m}$ ,  $180 - 425 \mu\text{m}$  and  $425 - 850 \mu\text{m}$ .  
17 Among the three CSDs, the largest particle size has never been directly obtained via  
18 crystallization. For the two smaller CSDs, the obtained size distribution has been not  
19 satisfactory.

20 Solubility data of azithromycin monohydrate and dihydrate crystals at different  
21 temperatures in pure acetone and in acetone/water mixtures are available in literature  
22 (shown in Figure 1).<sup>11</sup> In pure acetone, the solubility of dihydrate crystals is higher  
23 than that of monohydrates. Since the most stable polymorphic form has the lowest  
24 solubility<sup>24</sup>, monohydrate (microscopic image shown in Figure 2A) is the most stable  
25 form. However, in a mixture of acetone and water, this can change, the solubility of  
26 monohydrate can become higher and thus dihydrate (shown in Figure 2B) is the more  
27 stable form. As a result, as was found that dilution crystallization by adding water to  
28 the solution of azithromycin dissolved in acetone forms the metastable form  
29 monohydrates first. The monohydrates can then transform to dihydrates through  
30 solution mediated phase transition (SMPT)<sup>11</sup>. The key variables of the process are the

1 introduction of water as an anti-solvent and temperature reduction via cooling. The  
 2 aim is to use acetone/water mixture as the solvent to find the operational spaces that  
 3 produce azithromycin dihydrate crystals in the size ranges of  $< 180 \mu\text{m}$  ( $D_{50} = 78.3$   
 4  $\mu\text{m}$ ),  $180 - 425 \mu\text{m}$  ( $D_{50} = 155 \mu\text{m}$ ) and  $425 - 850 \mu\text{m}$  ( $D_{50} = 433 \mu\text{m}$ ). Previous  
 5 attempts were made (documents not available in the public domain) in industry and  
 6 by academia to achieve the objectives and proved this is very challenging, in  
 7 particular in making crystals in the size range  $425 - 850 \mu\text{m}$ .

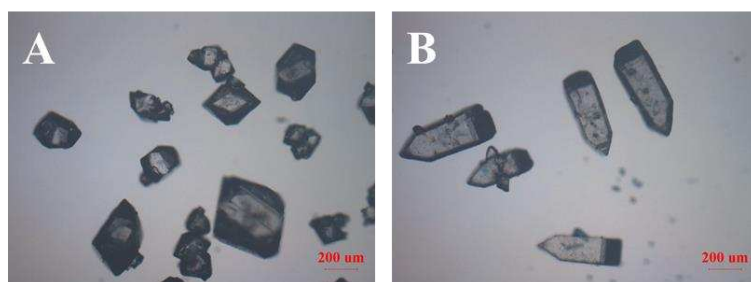
8



9

10 **Figure 1.** Molar fraction solubility of azithromycin as a function of temperature at different  
 11 water/acetone mixture compositions:<sup>11</sup> ■, monohydrate in 100% acetone; □, dihydrate in 100%  
 12 acetone; ▲, monohydrate in 90% acetone + 10% water; △, dihydrate in 90% acetone + 10%  
 13 water; ◆, monohydrate in 80% acetone + 20% water; ◇, dihydrate in 80% acetone + 20% water;  
 14 ★, monohydrate in 70% acetone + 30% water; ☆, dihydrate in 70% acetone + 30% water. ▼,  
 15 monohydrate in 60% acetone + 40% water; ▽, dihydrate in 60% acetone + 40% water.

16



17

18 **Figure 2.** Microscope images of azithromycin hydrates. A: monohydrate, B: dihydrate.

1

2 A 1 L jacketed reactor was firstly used for searching the operational spaces. An  
3 anchor impeller was used for gentle stirring at 100 rpm and the ratio of its height to  
4 the vessel filling height was always kept constant at one fourth. Pure acetone was the  
5 solvent and deionized water was the anti-solvent. The initial concentration was 0.5 g  
6 azithromycin dihydrate/g acetone at 40 °C. Then, 25% (w/w) water was introduced  
7 into the solution over 5 min. The temperature was first kept constant for 2 h and then  
8 dropped to 30 °C in 40 min. After that, 55% (w/w) water was added to the suspension  
9 in 2 h. The suspension was filtered, and the products obtained were then dried at  
10 65 °C overnight.

### 11 2.2.2 Real-time Concentration (Supersaturation) Measurement

12 ATR-FTIR Probe provided by Pharma Vision (Qingdao) Intelligent Technology  
13 Ltd was used for online measurement of azithromycin and water concentrations.  
14 Calibration experiments were designed to cover the following ranges: acetone/water  
15 mixtures containing 0 – 40 % (w/w) water, 0.01 – 0.6 g/g azithromycin, and  
16 temperatures between 20 – 40 °C. A partial least squares model was built using the  
17 calibration data. The peak at 1057 cm<sup>-1</sup> was used to quantify the azithromycin  
18 concentration and the ratio of the peaks at 3255 cm<sup>-1</sup> and 1710 cm<sup>-1</sup> was used to  
19 characterize the content of water in acetone. The optical fiber was then fixed and the  
20 probe was inserted in the same position within the crystallizer to avoid measurement  
21 errors throughout the entire set of experiments. With the solution concentration  
22 measured on-line in real-time, the supersaturation was calculated as:

$$23 \quad \beta = (C_i - C_s)/C_s \quad (1)$$

24 where  $\beta$  is the supersaturation (dimensionless),  $C_s$  is the saturated or equilibrium  
25 concentration and  $C_i$  is the immediate concentration of azithromycin in solution  
26 (acetone).

### 27 2.2.3 Monitoring of Crystal Growth Using On-line Imaging Technique

28 Online imaging has proved to be a useful tool for monitoring crystallization  
29 processes.<sup>16-18, 25-28</sup> Although accurate identification of the polymorphic form of  
30 crystals should be based on XRD, if the shape of two different polymorphs is very

1 different, on-line imaging can also be used for polymorph identification.<sup>27</sup> In this  
2 work, the 2D Vision Probe provided by Pharma Vision (Qingdao) Intelligent  
3 Technology Ltd was used for real-time qualitative and quantitative characterization of  
4 the shape and size of azithromycin crystals. The probe was immersed in the solution  
5 and connected to the specialized software called StereoVision CamSys so that crystal  
6 morphology images could be recorded. According to the sizes of the particles, the  
7 magnification can be adjusted to 2 times and 6 times. Due to a built-in ruler, the  
8 CamSys can accurately and rapidly perform multiscale segmentation of particles,  
9 thereby calculating particle shape parameters that could have physical meanings such  
10 as aspect ratio as well as latent shape descriptors such as shape descriptors defined by  
11 principal component analysis and Fourier transform.

#### 12 2.2.4 Crystal Size Distribution Characterization

13 The size distribution of dry crystals was measured using a Mastersizer 3000 laser  
14 diffraction particle size analyzer of Malvern Instruments Ltd. The dried azithromycin  
15 crystals were first introduced in the dry sample dispersion accessory and then  
16 measured by the analyzer. Each sample was measured three times. It is worth noting  
17 that the volume (or diameter) measured by Mastersizer 3000 is calculated based on a  
18 sphere. As shown in Figure 2, independent crystal faces and corner angles of the two  
19 types of crystal morphology can be observed distinctly. When the monohydrate  
20 crystals are observed in different directions (as shown in Figure 2A), the  
21 two-dimensional cross-section can be quadrilateral or hexagonal. The dihydrate  
22 crystals also show a certain aspect ratio (as shown in Figure 2B). Therefore, the two  
23 types of crystal morphologies are not spherical. Despite this fact, due to the relatively  
24 small aspect ratios of the two solid phases, they can be approximatively treated as  
25 spheres and thus measured by Mastersizer 3000.

26

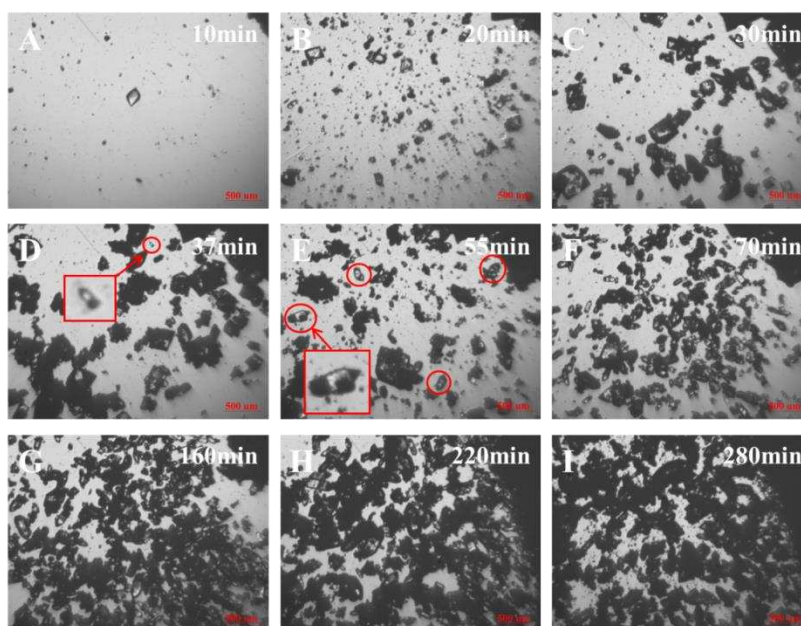
### 27 3. Results and Discussion

#### 28 3.1. Analyzing the Crystallization Process Using PAT

29 Coordinated utilization of ATR-FTIR and online imaging allows the study of the

1 multiple variables that affect the CSD. Moreover, unexpected deviations of the  
2 operation from the ideal situation during crystallization, such as partial transformation  
3 from monohydrate crystal to dihydrate crystals or no transformation, or unexpectedly  
4 high supersaturation due to unknown reason, can be detected in a timely manner by  
5 the PAT instrument, and immediate remedial adjustment can be made. Figure 3 shows  
6 examples of real-time images obtained. The changes in azithromycin concentration in  
7 the solution and supersaturation are shown in Figure 4.

8



9

10 **Figure 3.** Online images of the crystallization process taken at different times: A-C,  
11 azithromycin monohydrate nucleated and grew, no dihydrate was observed; D-F, azithromycin  
12 dihydrate nucleated and grew, while monohydrate gradually dissolved and eventually disappeared;  
13 G, as temperature decreased, the dihydrate crystals grew further; H and I, with the addition of  
14 water, crystal growth, secondary nucleation and aggregation were observed.

15

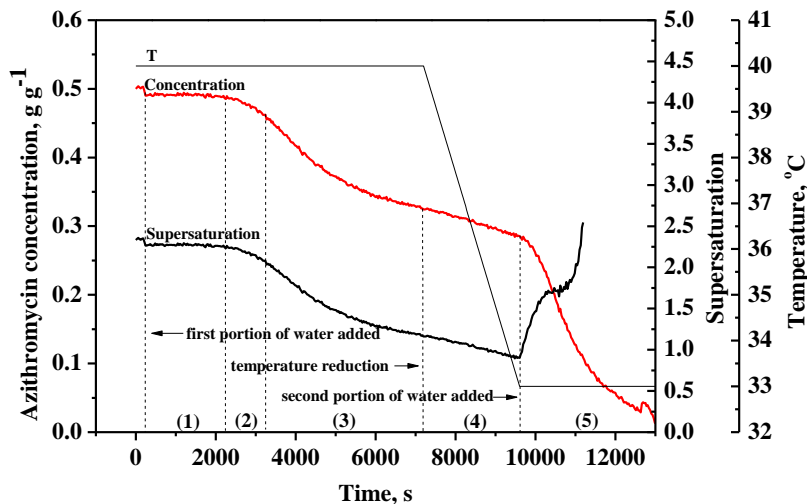


**Figure 4.** Azithromycin concentration (g/ (g acetone)), supersaturation and temperature in solution as a function of process time. The process can be divided into five sections as discussed in the body text.

Solution mediated phase transition (SMPT) can occur only from a less stable phase to a more stable phase, and the solution environment surrounding the solids affects the phase change.<sup>24</sup> In the current study of azithromycin crystallization in the mixture of acetone and water, azithromycin monohydrate is the less stable phase and the dihydrate is the more stable phase, and acetone/water mixture in which water acts as the anti-solvent provides a promoting environment for phase transition. For a dimorphic system, the SMPT involves at least three mechanisms:<sup>29</sup> primary nucleation of the more stable phase and the growth of both phases until the solubility of the metastable phase is reached, dissolution of the metastable phase, and growth of the more stable phase by mass transfer of solute in the solution. The three mechanisms coexist and are essential for the SMPT process. Thus, during the crystallization process, the polymorph transformation does not always proceed smoothly. In the azithromycin crystallization experiments, introduction of the first portion of water resulted in a relatively high initial supersaturation. Then, the concentration of azithromycin gradually decreased (shown in Figure 4, the region (1)), which resulted in the nucleation and growth of the monohydrate (shown in Figure 3A-C). Subsequently, the primary nucleation of dihydrate occurred and both solid phases grew (shown in Figure 3D-E), leading to a further decrease in concentration

1 (shown in Figure 4, the region (2)). With further decrease in concentration, the  
2 monohydrate solubility was reached and it started to dissolve while the dihydrate  
3 continued to nucleate and grow (shown in Figure 3E-F). After this point, change in  
4 concentration occurred due to the competing kinetics of dissolution of monohydrate  
5 and growth of dihydrate. The dissolution of monohydrate led to increase in  
6 concentration while the growth of dihydrate caused decrease in concentration. Since  
7 as shown in the region 3 of Figure 4, the concentration profile is decreasing although  
8 the gradient was sharper at first and then gradually became flat with time, it implies  
9 that the consumption of solute by growth of dihydrate is faster than the dissolution of  
10 monohydrate. Therefore, it can be deduced that dissolution of the monohydrate limits  
11 the transition and is the rate-controlling step. After this point, the dihydrate  
12 progressively grew and no monohydrate was observed (as shown in Figure 3G) as the  
13 temperature was decreased (coming to section (4) of Figure 4). With the introduction  
14 of the second portion of water (Figure 4, section (5)), fine particles and aggregation of  
15 crystals were observed.

16 The crystallization condition described above is viable for the completion of  
17 azithromycin hydrate transition. If any aberration occurs in the process, the transition  
18 might not be able to come to completion. The key factors are the amount of  
19 anti-solvent, and the ways the anti-solvent is introduced. More detailed discussion  
20 will be given in the next section.

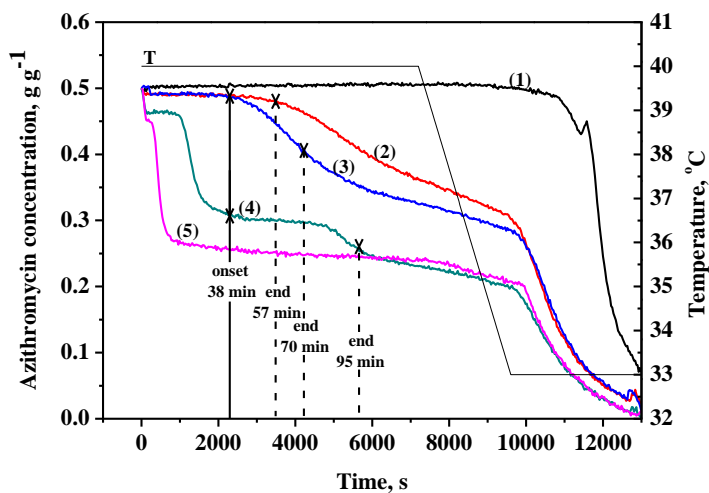
21

## 22 **3.2. The Influence of Anti-solvent**

### 23 3.2.1. The Amount of the First Portion of Water Added

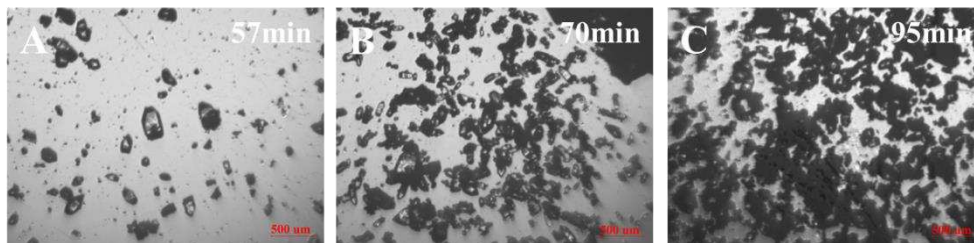
24 With the other conditions kept the same, the amount of the first portion of water  
25 added to the process was varied from 15% - 35% (w/w), and its effect on  
26 azithromycin crystallization was investigated. The changes in azithromycin  
27 concentration in the solution are shown in Figure 5. The real-time images of the  
28 crystallization solutions taken at the end of SMPT are shown in Figure 6. The crystal  
29 size distributions of the final products are shown in Figure 7.

30



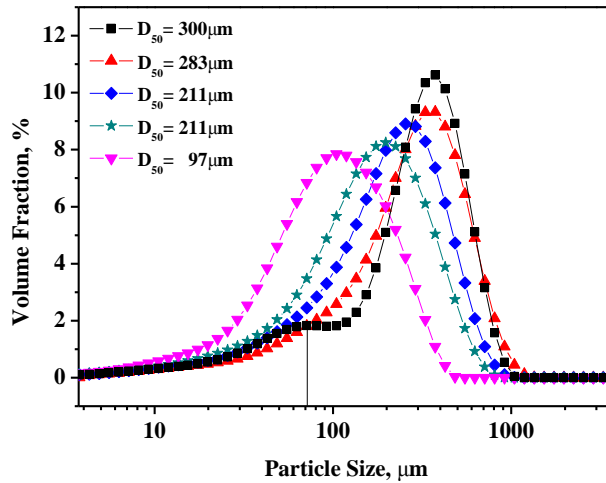
1  
2  
3  
4  
5  
6  
7

**Figure 5.** Azithromycin concentration (g / (g acetone)) and temperature in solution as a function of process time with different amounts of the first portion of added water: (1) 15%; (2) 20%; (3) 25%; (4) 30%; and (5) 35%. The solid line represents the onset of SMPT and the dashed lines refer to the end of SMPT.



8  
9  
10  
11  
12

**Figure 6.** Real-time images of the crystallization process taken at the end of polymorph transformation with different amounts of the first portion of added water: A, 20%; B, 25%; and C, 30%.



1  
2 **Figure 7.** Particle size distributions of the final products with different amounts of the first  
3 portion of added water: ■, 15%; ▲, 20%; ◆, 25%; ★, 30%; and ▼, 35%.

4  
5 The outcomes can be divided into three parts. For the case where 15% (w/w)  
6 water was added, when the crystals were large enough to be detected by the 2D  
7 Vision Probe, the observed crystals were already dihydrate so the SMPT process was  
8 not observed. This may be due to the high solubility of monohydrate when the water  
9 content is low. In other words, the monohydrate crystals have dissolved before they  
10 grew to a detectable size so that the onset and the end of SMPT cannot be judged.  
11 And for the case where 35% (w/w) water was added, as the concentration of the solid  
12 phase was too high, the morphologies of the crystals cannot be determined. So the  
13 SMPT process was not observed as well. However, when the amount of the first  
14 portion of water added to the process was varied from 20% - 30% (w/w), the SMPT  
15 processes were clearly observed and showed a certain pattern. Within this range, with  
16 the increase in the amount of added water, the first major drop in concentration  
17 showed sharper and earlier, as shown in Figure 5. This could be attributed to higher  
18 initial supersaturation, resulting in more nucleation of monohydrate crystals. Then the  
19 dihydrate crystals started nucleating in the solution almost at the same time for each  
20 condition at around 38 min. Subsequently, for each case where 20%, 25% and 30%  
21 (w/w) water was added, the monohydrate crystal was no longer observed at 57 min,  
22 70 min and 90 min (as shown in Figure 5 and 6), respectively. In other words, the  
23 transformation duration increased when more water was introduced in the mixtures.

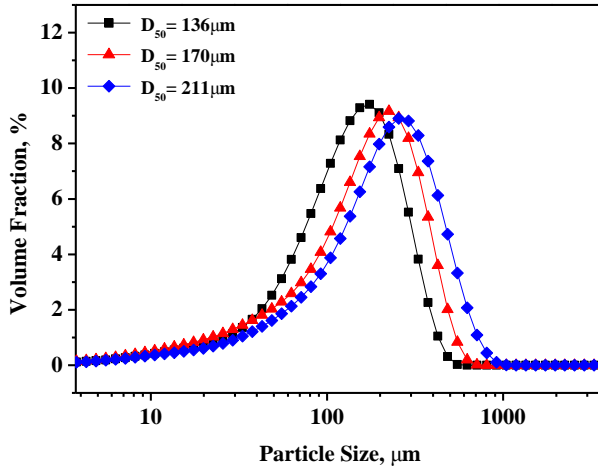
1 There could be two main reasons for this phenomenon. First, as mentioned above, the  
2 rate-controlling step of the azithromycin hydrate transformation is the dissolution of  
3 the monohydrate, and the increase in water content limits the dissolution. Second, the  
4 driving force of the process is the difference in solubility between the two types of  
5 hydrates. It can be seen from the solubility profiles that, when the proportion of water  
6 increases, the solubility difference becomes smaller until it is almost zero. Overall, the  
7 transformation duration is prolonged with increasing water content. Furthermore, it  
8 was observed that dihydrate crystals with larger numbers and smaller sizes were  
9 formed at the end of the hydrate transformation with higher supersaturation (as shown  
10 in Figure 6). After that point, the crystals continued to grow with subsequent cooling  
11 and the introduction of the second portion of water, and eventually formed the final  
12 products with different CSDs (as shown in Figure 7). Apparently, the smaller the  
13 amount of the first portion of water, the fewer the dihydrate crystals formed by  
14 primary nucleation, and therefore, the larger the average size of the final product. It  
15 can be seen that secondary nucleation occurred after the addition of the second  
16 portion of water, especially for 15% (w/w) water addition where a second peak was  
17 detected at around 73  $\mu\text{m}$  (as shown in Figure 7). Therefore, it can be concluded that  
18 the smaller the amount of the first portion of water, the larger the size of the final  
19 product, and the narrower the CSD. Nevertheless, this conclusion is only applicable to  
20 the range shown above. When the amount of added water was less than 10% (w/w),  
21 the supersaturation was not sufficient to induce nucleation until the temperature was  
22 reduced, thereby delaying the transformation. Also, as the transformation was limited  
23 by the second portion of water, the final product was a mixture of monohydrate and  
24 dihydrate. Therefore, in all the subsequent experiments, the amount of added water  
25 was always more than 10% (w/w). On the other hand, when the amount was larger  
26 than 40% (w/w), nearly all the solutes were consumed for the formation of  
27 monohydrate and no transformation occurred due to lowered driving force, resulting  
28 in no formation of dihydrate. Hence, through adjusting this parameter only, the  
29 controllable median particle diameter ( $D_{50}$ ) of the final product is 97 – 300  $\mu\text{m}$ .

1 3.2.2. The Feeding Rate of Water.

2 As mentioned above, if the amount of the first portion of water is insufficient, it  
3 might lead to only partial transformation from monohydrate to dihydrate crystals. It  
4 was also found that if the first portion of water was not introduced rapidly but  
5 introduced with a slow feeding rate, it could also result in only partial transformation  
6 from monohydrate to dihydrate crystals before the introduction of the second portion  
7 of water (though this part of result is not given here due to consideration of space  
8 limitation). Therefore, a relatively fast feeding rate for the first portion of water is  
9 necessary to ensure the completion of the hydrate transformation within the process  
10 duration.

11 The feeding rate of the second portion of water could have an impact on the final  
12 crystal size. Figure 8 shows the final CSDs measured by Mastersizer 3000 of three  
13 experiments corresponding to feeding rates of 0.5, 1.0, and 1.5% (w water /w  
14 acetone)/min respectively. For the three experiments, all other conditions are the same  
15 including the starting azithromycin concentration, the quantity of the first portion of  
16 water, the cooling rate as well as the total quantity of the second portion of water  
17 added. It is interesting to notice that the highest feeding rate 1.5% corresponds to the  
18 largest D50, while the lowest feeding rate is linked to the smallest D50. This  
19 experimental result could not be fully explainable. One speculative explanation is that  
20 the large particle size corresponding to 1.5% was due to aggregation of crystals  
21 induced by more small crystals formed as a result of secondary nucleation acting as  
22 bridges for crystals to aggregate. Please note, while in Figure 8, the Mastersizer 3000  
23 measurements did not show bimodal size distributions, the on-line imaging probe did  
24 show very clear fine particles in Figure 3I that was taken after the addition of the  
25 second portion of water.

26



1

2

**Figure 8.** Particle size distributions of the final products with different feed rates of second portion of added water: ■, 0.5%/min; ▲, 1.0%/min; and ◆, 1.5%/min.

4

### 3.3. The Influence of Temperature

6

7

8

9

10

11

12

13

14

15

16

17

18

19

20

21

22

23

As shown in Figure 3F-G, when the temperature was decreased, no nucleation was observed for the two types of hydrates. However, this does not indicate that temperature has no effect on the phase transition kinetics. In fact, it was found that it has a significant effect on the time required for completing the transition. At a lower temperature of 30 °C, a longer duration was required to accomplish the hydrate transformation (data not shown). Similarly, a higher temperature led to shorter transformation duration. This phenomenon can be explained by the mechanism of SMPT. The driving force of SMPT is the difference in solubility between the two polymorphs. As mentioned above, the rate-controlling step of the transition is the dissolution of the monohydrate. Therefore, at higher temperatures, the solubility of the monohydrate is higher while the difference in solubility is also greater, providing enhanced driving force and shortened transition duration. This explains why the polymorph transformation process needs to be carried out at higher temperatures. However, it also brings some setbacks. On the one hand, due to the dissolution characteristics of azithromycin, a single cooling method cannot guarantee sufficient crystallization yields. On the other hand, if dilution crystallization is continued, at a high temperature, it might cause excessive supersaturation which would subsequently bring about secondary nucleation and possible aggregation. Hence, a cooling step is

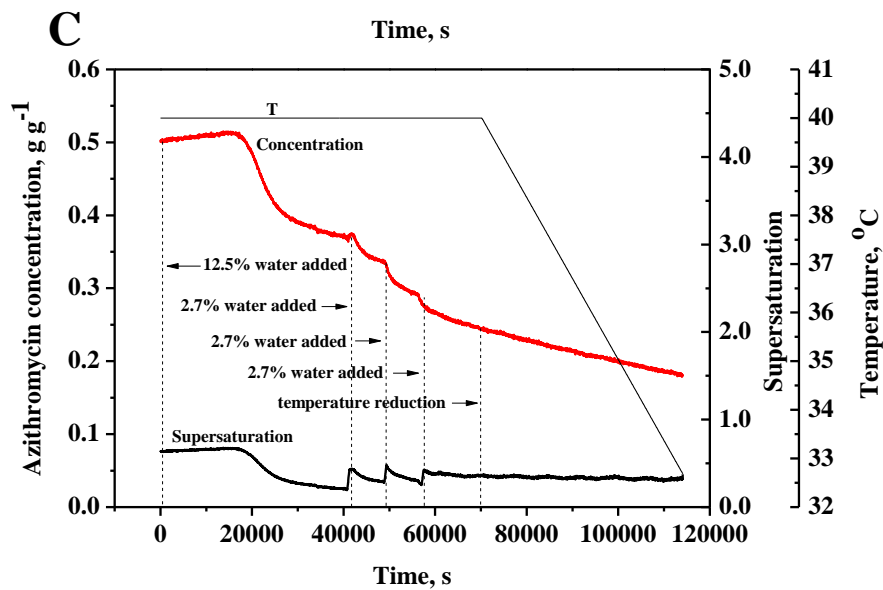
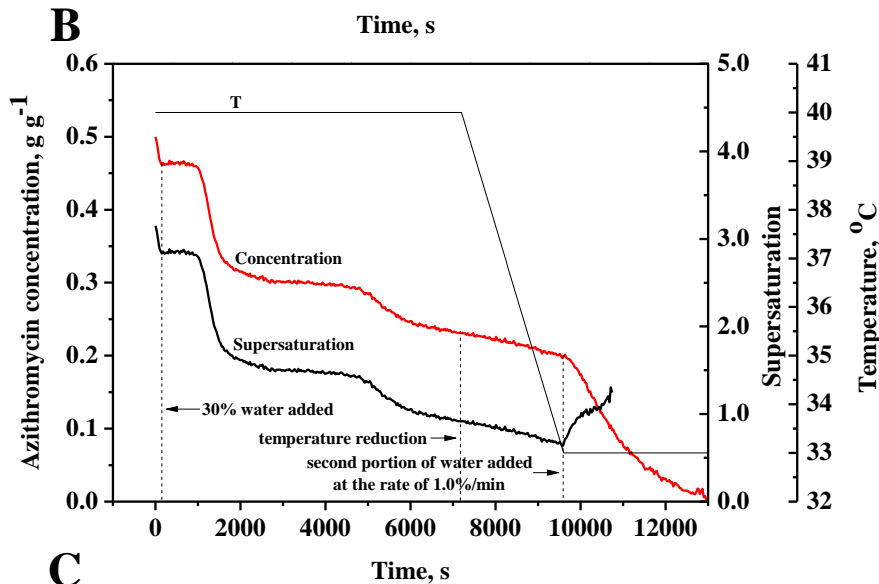
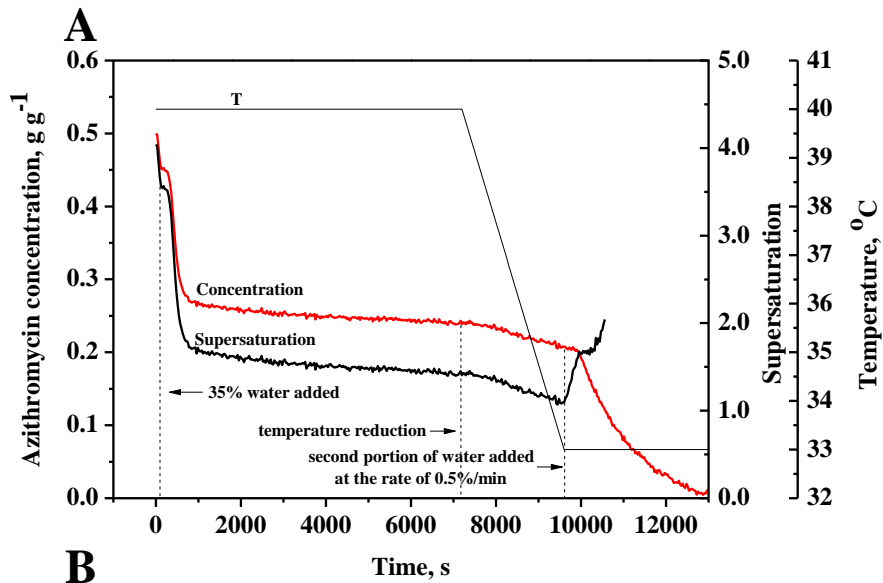
1 necessary prior to the second introduction of water to obtain a relatively low  
2 supersaturation and satisfactory yield. The cooling rate also has an effect on the  
3 crystal size of the final product. A slower cooling rate is preferred for larger particle  
4 size.

5

### 6 **3.4. The Operational Spaces Leading to Desired CSDs**

7 The results discussed above revealed that the key process variables to manipulate  
8 are the first portion of water, the cooling profile and the feeding profile of the second  
9 portion of water. The large number of experiments carried out with the aid of  
10 integrated PAT also resulted in identification of the operational spaces defined mainly  
11 by the three key variables that lead to tailored CSDs in the size ranges of  $< 180 \mu\text{m}$   
12 ( $D_{50} = 78.3 \mu\text{m}$ ),  $180 - 425 \mu\text{m}$  ( $D_{50} = 155 \mu\text{m}$ ) and  $425 - 850 \mu\text{m}$  ( $D_{50} = 433 \mu\text{m}$ ),  
13 in the mean time avoid abnormal operation such as excessive secondary nucleation,  
14 serious crystal aggregation, only partial phase transformation or no transformation  
15 from monohydrates to dihydrates. Below the three operational spaces and the crystal  
16 products obtained are introduced.

17 Figure 9A shows typical profiles of azithromycin solution concentration,  
18 temperature and supersaturation for a crystallization experiment that produces desired  
19 CSD in the size ranges of  $< 180 \mu\text{m}$  ( $D_{50} = 78.3 \mu\text{m}$ ). Figures 9B and 9C show  
20 concentration, temperature and supersaturation profiles of crystallization experiments  
21 that led to CSDs in the size ranges of  $180 - 425 \mu\text{m}$  ( $D_{50} = 155 \mu\text{m}$ ) and  $425 - 850$   
22  $\mu\text{m}$  ( $D_{50} = 433 \mu\text{m}$ ). Under the conditions of the three crystallization experiments of  
23 Figures 9A, 9B and 9C, the size distributions of the obtained crystals are shown in  
24 Figures 10A, 10B and 10C. Also shown in Figure 10 are the CSDs of three reference  
25 samples provided by the company. The reference samples were obtained via sieving.  
26 The microscope images of the crystals obtained in the three experiments are shown in  
27 Figures 11A, 11B and 11C. The conditions producing crystals in the three size ranges  
28 were obtained mainly by PAT aided experiments with guidance of crystallization  
29 knowledge. Below the crystallization conditions are introduced in more detail and  
30 attempts are made to give mechanistic and first-principle explanations.



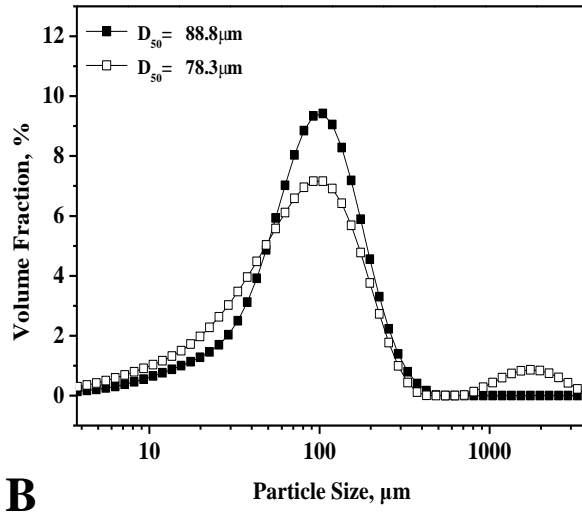
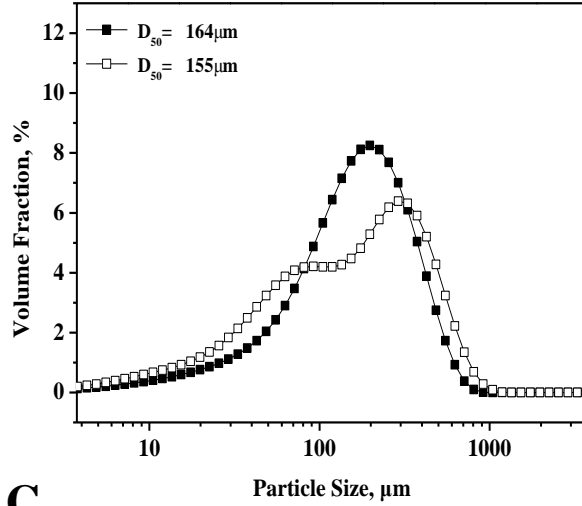
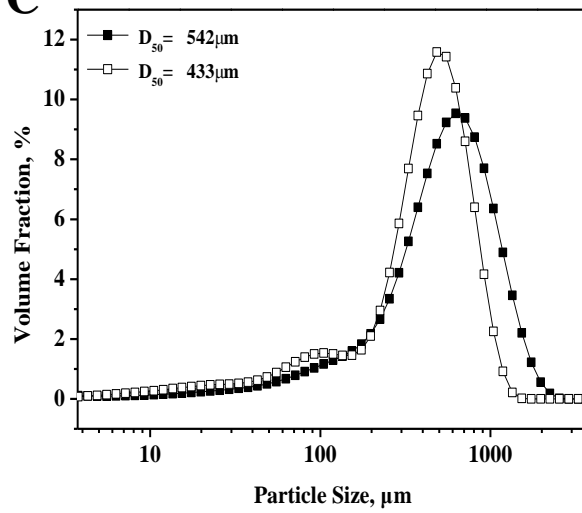
1 **Figure 9.** Azithromycin solution concentration (g / (g acetone)) , supersaturation and  
2 temperature profiles as a function of process time for obtaining products with different size ranges:  
3 A, < 180  $\mu\text{m}$ ; B, 180 – 425  $\mu\text{m}$ ; and C, 425 – 850  $\mu\text{m}$ .

#### 4 5 3.4.1 Production of crystals in the size range < 180 $\mu\text{m}$ ( $D_{50} = 78.3 \mu\text{m}$ )

6 The initial concentration was 0.5 g azithromycin dihydrate/g acetone. At 40 °C  
7 under continuous stirring in the reactor the crystals were fully dissolved. Then, the  
8 first portion of water, 35% (w water /w acetone), was added to the solution in 5  
9 minutes. This rapid introduction of water resulted in a high supersaturation of about 4,  
10 as depicted in Figure 9A at the start of the supersaturation profile. The supersaturation  
11 then rapidly dropped to slightly above 2 before became flat. The rapid drop of  
12 supersaturation from about 4 to about 2 is attributed to high nucleation rate due to the  
13 initial high supersaturation. High nucleation rate produces a large number of nuclei,  
14 which means small crystal size at the end of crystallization.

15 After the addition of the first portion of water, the temperature was maintained at  
16 40°C unchanged for about 2.3 hours. Then the crystallizer was linearly cooled from  
17 40°C down to 30°C in 40 minutes, before starting the introduction of the second  
18 portion of water. Based on observation using the on-line imaging probe, the transition  
19 from monohydrate to dihydrate crystals was completed prior to the start of adding the  
20 second portion of water. The second portion of water, 50% (w water /w acetone) , was  
21 added to the suspension in 100 minutes at a slow rate of 0.5% (w water /w  
22 acetone)/min to minimize secondary nucleation . As can be seen from Figure 10A, the  
23 obtained crystals have more uniform CSD, while the reference crystals show bimodal  
24 CSD.

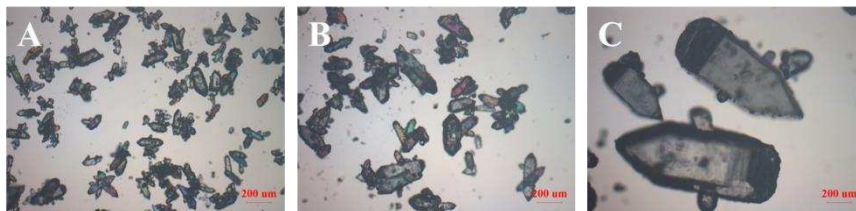
25

**A****B****C**

1 **Figure 10.** Crystal size distributions obtained in experiments in comparison with and  
2 reference samples, in crystal size ranges of: A, < 180  $\mu\text{m}$ ; B, 180 – 425  $\mu\text{m}$ ; and C, 425 – 850  $\mu\text{m}$ ;  
3 ■, products; □, reference samples.

#### 5 3.4.2 Production of crystals in the size range 180 – 425 $\mu\text{m}$ ( $D_{50} = 155 \mu\text{m}$ )

6 Optimization of the production of the crystals with the medium size range of 180  
7 – 425  $\mu\text{m}$  ( $D_{50} = 155 \mu\text{m}$ ) was relatively simple, as the required median particle  
8 diameter is within the controllable range (97 – 300  $\mu\text{m}$ ) by tuning only the amount of  
9 first portion of water. Hence, with other conditions the same as the original process  
10 described in Section 2.2, the amount of the first portion of water was altered to 30%  
11 (w/w). The initial supersaturation was high (as shown in Figure 9B) and the trend was  
12 similar to the original process (as shown in Figure 4). Dihydrate crystals were  
13 obtained (as shown in Figure 11B) with a median diameter ( $D_{50}$ ) of 164  $\mu\text{m}$ . Similarly,  
14 narrower and unimodal CSD was achieved (as shown in Figure 10B).



16  
17 **Figure 11.** Microscope images of the final products with different size ranges: A, < 180  $\mu\text{m}$ ; B,  
18 180 – 425  $\mu\text{m}$ ; and C, 425 – 850  $\mu\text{m}$ .

#### 20 3.4.3 Production of crystals in the size range 425 – 850 $\mu\text{m}$ ( $D_{50} = 433 \mu\text{m}$ )

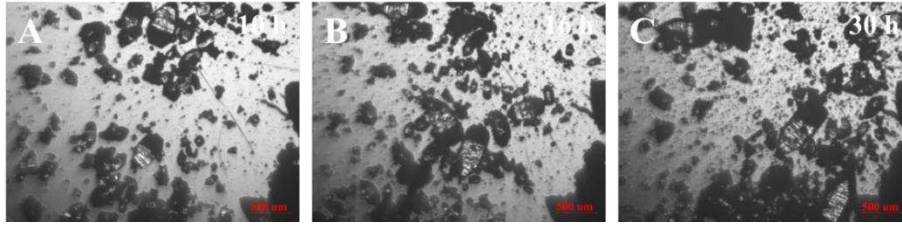
21 It was reported in literature that crystals in the range 425 – 850  $\mu\text{m}$  ( $D_{50} = 433 \mu\text{m}$ )  
22 were obtained via crystallization using ethyl acetate as the solvent<sup>11</sup>. However, this  
23 method is not yet approved by the China FDA. Thus, the preferred method in the  
24 company is still dilution crystallization in an acetone/water mixture. The  
25 crystallization condition that constantly produces crystals in the range 425 – 850  $\mu\text{m}$   
26 ( $D_{50} = 433 \mu\text{m}$ ) using acetone/water as the solvent is described below.

27 Starting from the same initial concentration as in producing the other two crystal

1 size ranges described in 3.4.1 and 3.4.2, and after all crystals were dissolved at 40<sup>0</sup>C,  
2 12.5% water (w water /w acetone) was added to the solution. The supersaturation was  
3 measured as 0.6 (as shown in Figure 9C), at such a low supersaturation, nucleation  
4 rate should not be high. On the supersaturation profile in Figure 9C, there was no  
5 immediate and rapid reduction of supersaturation after the water addition. This is  
6 unlike the previous two cases shown in Figures 9A and 9B where very sharp drop of  
7 supersaturation after the addition of the first portion of water was seen. It is assumed  
8 in this occasion, a much smaller number of crystals were formed. Then, with the  
9 consumption of solute, the supersaturation gradually decreased. In here it needs to  
10 point out that if the water added is less than 12.5%, it might not generate  
11 supersaturation high enough to trigger nucleation, as discussed in Section 3.2.1 where  
12 10% water (w/w) was added and nucleation was only observed after the temperature  
13 started to decrease.

14 Also unlike the conditions to produce crystals of the other two size ranges,  
15 production of crystals in the size range 425 – 850  $\mu\text{m}$  requires introduction of water in  
16 multiple batches before coming to the stage of temperature reduction via cooling. As  
17 marked in Figure 9C, after introduction of 12.5% water (w water /w acetone), further  
18 water was added at 42000s, 49000s and 58000s, each time, 2.7% water (w/w) was  
19 introduced. Figures 12A and 12B captured images of growing crystals at 36000s and  
20 57600s. Temperature reduction from 40<sup>0</sup>C to 30<sup>0</sup>C started at 70000s, as shown in  
21 Figure 9C, at a very slow cooling rate of 0.01<sup>0</sup>C/min to maintain a nearly constant  
22 supersaturation. Subsequently, 60% water (w water / w acetone) was added to the  
23 solution at a rate of 1.5% water (w water / w acetone)/min. At the end, large dihydrate  
24 crystals with a median diameter ( $D_{50}$ ) of 542  $\mu\text{m}$  were observed. A microscope image  
25 of crystals is shown in Figure 11C, CSD comparison with the reference sample is  
26 shown in Figure 10C. The crystals satisfied the company and company's customer's  
27 requirement.

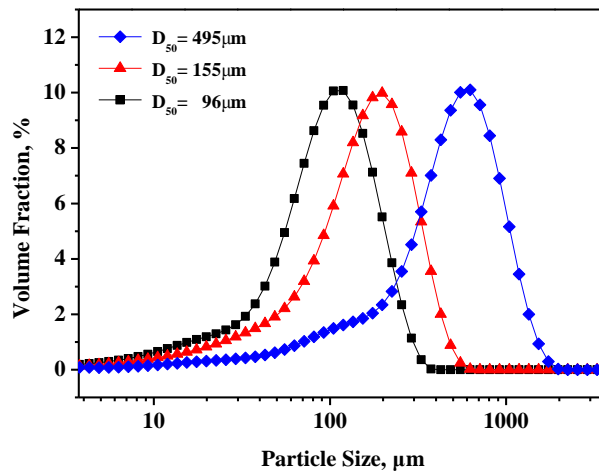
28



1  
2 **Figure 12.** Online images of the crystallization solution taken at different times: A, 10 h; B, 16 h;  
3 and C, 30 h.

### 6 3.5. Scale-up

7 The operational spaces derived in the 1 L reactor were then validated in a 25 L  
8 crystallizer. According to the principle of scale-up based on constant tip speed, the  
9 stirring speed was set to 48 rpm. The CSDs of the final products are shown in Figure  
10 13.



11  
12  
13 **Figure 13.** Particle size distributions of the final products obtained in the 25 L crystallizer with  
14 different size ranges: ■, < 180 μm; ▲, 180 – 425 μm; and ◆, 425 – 850 μm.

15  
16 Similar results were obtained when the same three operating conditions were  
17 applied on the 25 L scale. Dihydrate crystals and a few clusters were formed and no  
18 monohydrate was observed. Similar median diameters were achieved while the  
19 unimodal CSDs of the 25 L scale were even narrower than those of the 1 L scale. The  
20 sieving outcomes of the final products were in line with practical production  
21 requirements.

## 1 **4. Conclusion**

2 Combined use of on-line imaging and ATR FTIR instrument allowed the direct  
3 observation and real-time measurement of azithromycin polymorph transition from  
4 monohydrate to dihydrate crystals and crystal growth behavior at different operating  
5 conditions in the acetone/water system. Factors affecting the transition and crystal  
6 size distribution of the final product were identified and quantified. Within a certain  
7 range, smaller amount of the first portion of water addition resulted in larger crystal  
8 size and narrower CSD. Outside this range, partial or even no transition occurred.  
9 Additionally, when the feed rate of the second portion of water was increased, a larger  
10 average crystal size was obtained. Furthermore, higher temperature was found to be  
11 conducive to polymorph transition and slower cooling rate was favorable for the  
12 crystal growth. Based on the insights obtained into the causal relationships between  
13 the multiple variables and crystal growth behavior, the operational spaces leading to  
14 the three desired CSDs were defined as follows: the initial concentration of 0.5g  
15 azithromycin dihydrate/g acetone at 40 °C was kept the same. (1) 35% (w/w) water  
16 was introduced in the solution over 5 min. The temperature was first kept constant for  
17 2 h and then dropped to 30 °C in 40 min. After that, 50% (w/w) water was added to  
18 the suspension at the rate of 0.5% (by weight of pure acetone)/min; (2) 30% (w/w)  
19 water was introduced in the solution over 5 min. The temperature was first kept  
20 constant for 2 h and then dropped to 30 °C in 40 min. After that, 55% (w/w) water  
21 was added to the suspension at the rate of 1.5% (by weight of pure acetone)/min; (3)  
22 12.5% (w/w) water was first added over 5 min. Then 2.7% (w/w) water was added  
23 over 1 min every 2.5 h thrice. After that, the temperature was reduced to 30 °C at the  
24 rate of 0.01 °C /min. Then, 60% (w/w) water was added to the solution at the rate of  
25 1.5% (by weight of pure acetone)/min. By adopting these conditions, dihydrate  
26 products with the three desired CSDs were obtained in a 1 L crystallizer. The  
27 developed process allowed for streamlined steps and cost reduction compared to the  
28 current sieving method, especially for the largest size range of 425 – 850 µm. The  
29 crystallization processes were then successfully scaled-up to 25 L with comparable

1 results, validating the operational spaces.

2 The discussion in this paper has focused on the use of PAT in revealing the  
3 complex relationships between the multi-factorial process conditions and product  
4 specifications in azithromycin crystallization, which as pointed out by Read et al.<sup>30, 31</sup>  
5 is a key component of PAT. Successful use of PAT in industry should be able to make  
6 use of the on-line measurements to exercise closed-loop control.<sup>30, 31</sup> As the next  
7 phase of the work, we are working on the automatic closed-loop control of the process  
8 and will report the outcome in due course.

9

## 10 **Acknowledgements**

11 This work was financially supported by the National Natural Science Foundation  
12 of China (NNSFC) under its Major Research Scheme of Mesoscale Mechanism and  
13 Control in Multiphase Reaction Processes (grant reference: 91434126), the Natural  
14 Science Foundation of Guangdong Province (grant reference: 2014A030313228), the  
15 Guangdong Provincial Science and Technology Projects under the Scheme of Applied  
16 Science and Technology Research Special Funds (grant reference: 2015B020232007),  
17 as well as the pharmaceutical company whose name cannot be disclosed due to  
18 confidentiality agreement. The authors would like to extend their thanks to Dr Jianguo  
19 Cao of Pharmavision (Qingdao) Intelligent Technology Limited (www.pharmavision  
20 -ltd.com) who provided assistance in the imaging and the ATR FTIR instrument.

21

## 22 **References**

- 23 1. Dunn, C. J.; Barradell, L. B., Azithromycin. A review of its pharmacological  
24 properties and use as 3-day therapy in respiratory tract infections. *Drugs* **1996**, *51*,  
25 483-505.
- 26 2. Langtry, H. D.; Balfour, J. A., Azithromycin - A review of its use in paediatric.  
27 *Drugs* **1998**, *56*, 273-297.
- 28 3. Mandell, L. A.; Wunderink, R. G.; Anzueto, A.; Bartlett, J. G.; Campbell, G. D.;  
29 Dean, N. C.; Dowell, S. F.; Jr, F. T.; Musher, D. M.; Niederman, M. S., Infectious  
30 Diseases Society of America/American Thoracic Society consensus guidelines on the

- 1 management of community-acquired pneumonia in adults. *Clinical Infectious*  
2 *Diseases* **2007**, 44 Suppl 2, S27-S72.
- 3 4. Woodhead, M.; Blasi, F.; Ewig, S.; Huchon, G.; Leven, M.; Ortqvist, A.; Ieven,  
4 M.; Schaberg, T.; Torres, A.; van der Heijden, G., Guidelines for the management of  
5 adult lower respiratory tract infections. *European Respiratory journal* **2005**, 26,  
6 1138-1180.
- 7 5. Singer, C.; Aronhime, J. Ethanolate of azithromycin, process for manufacture,  
8 and pharmaceutical compositions thereof. US6365574B2, 2002.
- 9 6. Kotliar, E. M.; Hrakovsky, J.; Tenengauzer, R. Azithromycin powder for oral  
10 suspension compositions. EP1855693B1, 2009.
- 11 7. Bayod, J. M. S.; Garcia, I. L.; Mari, F. F. Azithromycin preparation in its  
12 noncryst alline and crystalline dihydrate forms. US6451990B1, 2002.
- 13 8. Sundaramurthi, P.; Suryanarayanan, R., Azithromycin hydrates-implications of  
14 processing-induced phase transformations. *Journal of Pharmaceutical Sciences* **2014**,  
15 103, 3095-106.
- 16 9. Adeli, E.; Mortazavi, S. A., Design, formulation and evaluation of Azithromycin  
17 binary solid dispersions using Kolliphor series for the solubility and in vitro  
18 dissolution rate enhancement. *Journal of Pharmaceutical Investigation* **2014**, 44,  
19 119-131.
- 20 10. Ma, B.; Gong, J., Optimization of Crystallization Process of Azithromycin  
21 Dihydrate. *Chemical Industry and Engineering (Tianjin, China)* **2015**, 32, 37-40.
- 22 11. Wu, S.; Shen, H.; Li, K.; Yu, B.; Xu, S.; Chen, M.; Gong, J.; Hou, B.,  
23 Agglomeration mechanism of azithromycin dihydrate in acetone-water mixtures and  
24 optimize the powder properties. *Industrial & Engineering Chemistry Research* **2016**,  
25 55, 112-117.
- 26 12. Li, F.; Wu, Z.; Wang, W. Azithromycin direct crystallization in aqueous phase  
27 includes preparing sodium hydroxide solution and dropping into aqueous solution of  
28 azithromycin salt while stirring, cooling, and crystallizing. CN102911219A, 2013.
- 29 13. Bayod, J. M. S.; Garcia, I. L.; Mari, F. F. Preparation of crystalline azithromycin  
30 dihydrate. EP1234833B1, 2006.
- 31 14. Allen, D. J. M.; Nepveux, K. M. Dihydrate de l'azithromycine. EP0298650A2,  
32 1989.
- 33 15. Pshenichnikov, V. G.; Rabinovich, I. M.; Zaripova, Z. I. Method for crystallizing  
34 azithromycin dihydrate provides enhancing stability and homogeneity of the end  
35 crystalline product. RU2260012C1, 2005.

- 1 16. Nagy, Z. K.; Fevotte, G.; Kramer, H.; Simon, L. L., Recent advances in the  
2 monitoring, modelling and control of crystallization systems. *Chemical Engineering*  
3 *Research and Design* **2013**, 91, 1903-1922.
- 4 17. Wu, H. Q.; Dong, Z. D.; Li, H. T.; Khan, M., An Integrated Process Analytical  
5 Technology (PAT) Approach for Pharmaceutical Crystallization Process  
6 Understanding to Ensure Product Quality and Safety: FDA Scientist's Perspective.  
7 *Organic Process Research and Development* **2015**, 19, 89-101.
- 8 18. Simon, L. L.; Pataki, H.; Marosi, G.; Meemken, F.; Hungerbuhler, K.; Baiker, A.;  
9 Tummala, S.; Glennon, B.; Kuentz, M.; Steele, G.; Kramer, H. J. M.; Rydzak, J. W.;  
10 Chen, Z. P.; Morris, J.; Kjell, F.; Singh, R.; Gani, R.; Gernaey, K. V.; Louhi-Kultanen,  
11 M.; O'Reilly, J.; Sandler, N.; Antikainen, O.; Yliruusi, J.; Frohberg, P.; Ulrich, J.;  
12 Braatz, R. D.; Leyssens, T.; von Stosch, M.; Oliveira, R.; Tan, R. B. H.; Wu, H. Q.;  
13 Khan, M.; O'Grady, D.; Pandey, A.; Westra, R.; Delle-Case, E.; Pape, D.;  
14 Angelosante, D.; Maret, Y.; Steiger, O.; Lenner, M.; Abbou-Oucherif, K.; Nagy, Z. K.;  
15 Litster, J. D.; Kamaraju, V. K.; Chiu, M. S., Assessment of Recent Process Analytical  
16 Technology (PAT) Trends: A Multiauthor Review. *Organic Process Research and*  
17 *Development* **2015**, 19, 3-62.
- 18 19. Zhang, H. T.; Lakerveld, R.; Heider, P. L.; Tao, M. Y.; Su, M.; Testa, C. J.;  
19 D'Antonio, A. N.; Barton, P. I.; Braatz, R. D.; Trout, B. L.; Myerson, A. S.; Jensen, K.  
20 F.; Evans, J. M. B., Application of Continuous Crystallization in an Integrated  
21 Continuous Pharmaceutical Pilot Plant. *Crystal Growth & Design* **2014**, 14,  
22 2148-2157.
- 23 20. Hansen, T. B.; Simone, E.; Nagy, Z.; Qu, H. Y., Process Analytical Tools To  
24 Control Polymorphism and Particle Size in Batch Crystallization Processes. *Organic*  
25 *Process Research and Development* **2017**, 21, 855-865.
- 26 21. Gomes, J.; Chopda, V. R.; Rathore, A. S., Integrating systems analysis and  
27 control for implementing process analytical technology in bioprocess development.  
28 *Journal Of Chemical Technology And Biotechnology* **2015**, 90, 583-589.
- 29 22. Stelzer, T.; Wong, S. Y.; Chen, J.; Myerson, A. S., Evaluation of PAT Methods  
30 for Potential Application in Small-Scale, Multipurpose Pharmaceutical Manufacturing  
31 Platforms. *Organic Process Research and Development* **2016**, 20, 1431-1438.
- 32 23. Ma, C. Y.; Liu, J. J.; Wang, X. Z., Measurement, modelling, and closed-loop  
33 control of crystal shape distribution: Literature review and future perspectives.  
34 *Particuology* **2016**, 26, 1-18.
- 35 24. Mangin, D.; Puel, F.; Veesler, S., Polymorphism in Processes of Crystallization  
36 in Solution: A Practical Review. *Organic Process Research and Development* **2009**,  
37 13, 1241-1253.

- 1 25. Wang, X. Z.; Roberts, K. J.; Ma, C., Crystal growth measurement using 2D and  
2 3D imaging and the perspectives for shape control. *Chemical Engineering Science*  
3 **2008**, 63, 1173-1184.
- 4 26. De Anda, J. C.; Wang, X. Z.; Roberts, K. J., Multi-scale segmentation image  
5 analysis for the in-process monitoring of particle shape with batch crystallisers.  
6 *Chemical Engineering Science* **2005**, 60, 1053-1065.
- 7 27. De Anda, J. C.; Wang, X. Z.; Lai, X.; Roberts, K. J.; Jennings, K. H.; Wilkinson,  
8 M. J.; Watson, D.; Roberts, D., Real-time product morphology monitoring in  
9 crystallization using imaging technique. *Aiche Journal* **2005**, 51, 1406-1414.
- 10 28. Borsos, A.; Szilagyi, B.; Agachi, P. S.; Nagy, Z. K., Real-Time Image Processing  
11 Based Online Feedback Control System for Cooling Batch Crystallization. *Organic*  
12 *Process Research and Development* **2017**, 21, 511-519.
- 13 29. Cardew, P. T.; Davey, R. J., The Kinetics of Solvent-Mediated Phase  
14 Transformations. *Proceedings of the Royal Society A Mathematical Physical and*  
15 *Engineering Sciences* **1985**, 398, 415-428.
- 16 30. Read, E. K.; Park, J. T.; Shah, R. B.; Riley, B. S.; Brorson, K. A.; Rathore, A. S.,  
17 Process Analytical Technology (PAT) for Biopharmaceutical Products: Part I.  
18 Concepts and Applications. *Biotechnology and Bioengineering* **2010**, 105, 276-284.
- 19 31. Read, E. K.; Park, J. T.; Shah, R. B.; Riley, B. S.; Brorson, K. A.; Rathore, A. S.,  
20 Process Analytical Technology (PAT) for Biopharmaceutical Products: Part II.  
21 Concepts and Applications. *Biotechnology and Bioengineering* **2010**, 105, 285-295.

22

23 **TOC Graphic**



A, < 180  $\mu\text{m}$

B, 180 – 425  $\mu\text{m}$

C, 42 – 850  $\mu\text{m}$

